Helicity-dependent all-optical domain wall motion in ferromagnetic thin films

Y. Quessab, R. Medapalli, M S El Hadri, M. Hehn, G. Malinowski, E. E. Fullerton, S. Mangin

Helicity-dependent all-optical domain wall motion in ferromagnetic thin films

Y. Quessab,[1,2,*] R. Medapalli,[2] M. S. El Hadri,[1] M. Hehn,[1] G. Malinowski,[1] E. E. Fullerton,[2] and S. Mangin[1]
[1]*Institut Jean Lamour, UMR CNRS 7198, Université de Lorraine, Boîte Postale 70239, F-54506 Vandoeuvre-lès-Nancy, France*
[2]*Center for Memory and Recording Research, University of California, San Diego, La Jolla, California 92093-0401, USA*

(Received 6 September 2017; revised manuscript received 15 November 2017; published 20 February 2018)

Domain wall displacement in Co/Pt thin films induced by not only femtosecond but also picosecond laser pulses is demonstrated using time-resolved magneto-optical Faraday imaging. We evidence multipulse helicity-dependent laser-induced domain wall motion in all-optical switchable Co/Pt multilayers with a laser energy below the switching threshold. Domain wall displacement of ∼2 nm per 2-ps pulse is achieved. By investigating separately the effect of linear and circular polarization, we reveal that laser-induced domain wall motion results from a complex interplay between pinning, temperature gradient, and helicity effect. Then, we explore the microscopic origin of the helicity effect acting on the domain wall. These experimental results enhance the understanding of the mechanism of all-optical switching in ultrathin ferromagnetic films.

DOI: 10.1103/PhysRevB.97.054419

I. INTRODUCTION

Magnetization manipulation based on ultrashort laser pulses without any external magnetic field has recently attracted researchers' attention as it could lead to ultrafast and high-density magnetic data storage [1,2]. In 2007, it was shown that the magnetization of a ferrimagnetic GdFeCo alloy could be fully reversed on a picosecond time scale using circularly polarized light [3]. Thus, all-optical switching (AOS) rapidly became a topic of great interest. It was observed in a wider variety of materials ranging from ferrimagnetic multilayers and heterostructures and rare-earth (RE)-free synthetic ferrimagnetic heterostructures [4,5] to ferromagnetic continuous thin films and granular media [6,7]. Unlike GdFeCo alloys for which all-optical magnetization reversal is said to result from a purely thermal process [8–10], several mechanisms and microscopic models based on the inverse Faraday effect (IFE) or magnetic circular dichroism (MCD) were proposed to explain all-optical helicity-dependent magnetization switching (AO-HDS) in ferromagnetic materials [11,12]. Furthermore, single-pulse optical excitation of Pt/Co/Pt only leads to thermal demagnetization [13]. Thus, the latter indicates that in ferromagnetic systems, all-optical switching is rather a cumulative and multipulse mechanism [7,13,14] with two regimes: a demagnetization and a multidomain state followed by a helicity-dependent remagnetization assumed to result from domain wall (DW) motion which depends upon the light helicity [13,14].

In continuous magnetic media, a DW separates two magnetic domains of uniform and opposite magnetization. Domain walls, with their high mobility, are of great interest for low-power spintronic applications, such as racetrack memories [15] and logic devices [16,17]. Magnetic-field-driven DW motion in ferromagnets with strong perpendicular anisotropy, such as ultrathin Pt/Co/Pt films, has been extensively studied [18]. Current-induced DW motion in ferromagnetic elements, via spin-transfer torque (STT), was also reported [19,20]. Control of the DW by electric field [21], voltage-induced strain [22], and thermal gradients by either injecting current [23] or local heating [24–26] are other possibilities for manipulation of DW. In this paper, we report deterministic motion of domain walls in Co/Pt multilayers that show AO-HDS, using circularly polarized laser pulses. We have investigated the DW displacement as a function of laser polarization, beam position, and laser power. The results reveal that the physical mechanism differs from pure thermal-gradient-driven DW motion. Instead, it arises from the balance of three contributions: pinning, heating, and helicity. The inverse Faraday effect and magnetic circular dichroism are two models explored to elucidate the effect of helicity on the DW. These findings can be key elements to explain magnetization reversal in AOS.

II. SAMPLES AND EXPERIMENTAL METHODS

Two ferromagnetic (Co/Pt) multilayers were studied: glass/Ta(5)/Pt(5)/$[Co(0.4)/Pt(0.7)]_{x3}$/Pt(2) and glass/Ta(5)/Pt(4.5)/Co(0.6)/Pt(0.7)/Pt(3.8) (the parentheses show thickness in nanometers). These thin films were both grown by dc magnetron sputtering. The bottom Ta/Pt bilayer allows good adherence of the multilayer stack on the glass substrate and a (111) texture of the (Co/Pt) layers, which ensures perpendicular magnetic anisotropy (PMA) and a high-anisotropy field [27]. The top Pt layer prevents sample oxidation.

To perform optical excitation and AO-HDS, two different ultrafast laser systems were used. On the one hand, the Pt/Co/Pt single-layer sample was exposed to a Ti:sapphire femtosecond laser with a 5-kHz repetition rate, a central wavelength of 800 nm, and a pulse duration τ_{pulse} of 40 fs. The laser beam spot has a Gaussian profile and is focused on the sample surface with a full width at half maximum (FWHM) of 50 μm. On the other hand, a $Pt/[Co/Pt]_{x3}/Pt$ trilayer thin film was excited by 2-ps, 800-nm laser pulses with a repetition rate of 1 kHz and a Gaussian beam spot with a FWHM of 45 μm. Right-circularly (σ^+), left-circularly (σ^-), or linearly (π)

*yassine.quessab@univ-lorraine.fr

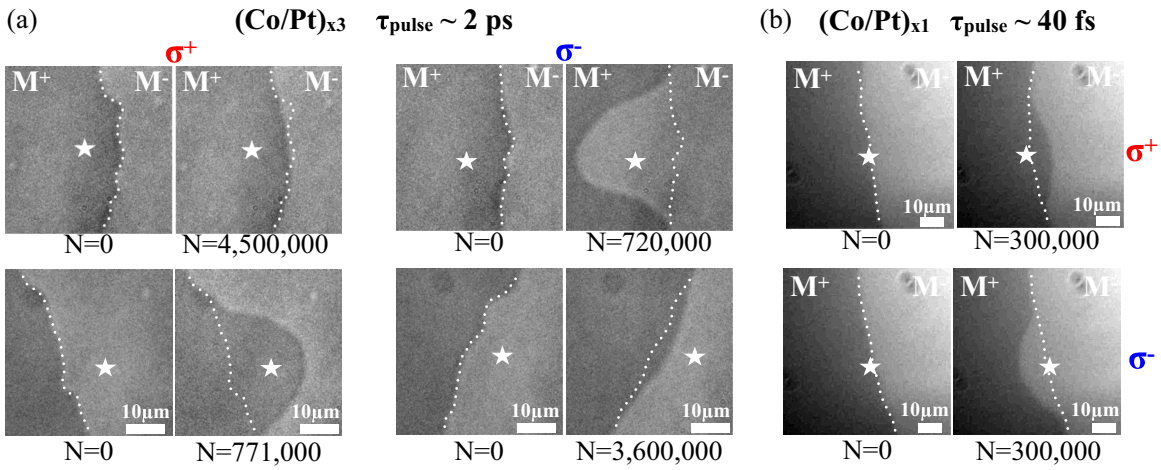

FIG. 1. Magneto-optical images of domain wall motion in $[Co(0.4\ nm)/Pt(0.7\ nm)]_{x3}$ and $[Co(0.6\ nm)/Pt(0.7\ nm)]_{x1}$ induced, respectively, by (a) 2-ps and (b) 40-fs laser pulses with left-circular (σ^-) and right-circular (σ^+) polarization with an energy per pulse of 0.04 and 12.5 mJ cm^{-2}. The white star indicates the center of the beam spot, and N is the number of laser pulses. The laser beam spot is (a) placed 10 μm away from the DW within a magnetization-up (M^+) or -down (M^-) domain or (b) centered on the wall. The dotted line shows the initial position of the domain wall prior to laser exposure.

polarized light is obtained with the use of a polarizer combined with a quarter-wave plate (QWP). These two ferromagnetic multilayer films, Pt/Co/Pt single and trilayer, were extensively studied, and they both exhibit AO-HDS with 40-fs and 2-ps laser pulses, respectively [6,13,14,28]. Thus, our aim was to investigate in these two Co/Pt structures the mechanism of the helicity-dependent magnetization recovery described by El Hadri *et al.* [13]. In our experiments, the pulse duration was chosen according to the Co/Pt system so that the conditions were the same as in [13,14], which give AOS. To study the laser-induced domain wall motion, we implemented a magneto-optical Faraday imaging technique as a function of time and number of laser pulses N. To probe the effect of the optical excitation of the DW, a Faraday microscope was used, and a CCD camera was used to take an image every second.

Prior to the DW motion experiments, all-optical switching of the films was first verified by sweeping the laser beam over the sample surface. We determined the power threshold for which AO-HDS is observed (0.044 mJ cm^{-2} for Pt/$[Co/Pt]_{x3}$/Pt and 14.5 mJ cm^{-2} for the Pt/Co/Pt single layer). Afterwards, an external magnetic field perpendicular to the sample surface is applied to set the magnetization in the "up" (M^+) direction, which corresponds to dark contrast on Faraday images. Then, a reversed magnetic domain (M^-, bright contrast) is created. During all DW motion experiments, no magnetic field is applied to the sample, and the laser pump comes at normal incidence on the sample surface. The center of the laser beam, i.e., the maximum of intensity, is placed at different positions with respect to the DW with a translational stage with micron precision.

III. RESULTS

A. Femtosecond- and picosecond-laser-induced domain wall motion in Co/Pt thin films

As already mentioned, it was recently demonstrated that the Pt(4.5)/Co(0.6)/Pt(4.5) single layer and Pt(5)/$[Co(0.4)/Pt(0.7)]_{x3}$/Pt(2) trilayer showed AO-HDS with femtosecond and picosecond laser pulses, respectively, via electrical Hall measurements or static imaging after laser beam sweeping [6,14,28]. Note that Pt/$[Co/Pt]_{x3}$/Pt when excited with 40-fs laser pulses does not show AOS but instead only thermal demagnetization. First, we investigated whether we could observe DW motion in these materials with laser pulses of the same duration as those leading to AO-HDS (see Fig. 1). DW experiments were performed at a fluence lower than the switching threshold so that no reversed magnetic domain is observed. Therefore, the changes in the DW pattern in Fig. 1 can be attributed only to DW motion and not to domain nucleation. Figure 1(a) shows the evolution of the DW in Pt/$[Co/Pt]_{x3}$/Pt after being exposed to circularly polarized light. The center of the laser beam spot is placed 10 μm from the DW on a domain with either magnetization up (M^+) or magnetization down (M^-). Thus, four combinations of light polarization and position of laser beam, (σ^+, M^+), (σ^+, M^-), (σ^-, M^+), and (σ^-, M^-), were studied. Note that the laser beam spot overlaps both magnetic domains, yet what is important is the position of the maximum of intensity, i.e., the location of the hottest region with regard to the DW. When clear DW displacement (DWD) was observed, image recording was stopped after stabilization of the DW. The experiments were repeated several times, each time on a different area that had not previously been exposed to the laser beam. Only two combinations, (σ^+, M^-) and (σ^-, M^+), led to significant DW displacement. As seen in Fig. 1(a), when a M^- domain is exposed to σ^+ pulses, the DW moves in such a way that the M^+ domain expands. Conversely, a M^+ domain illuminated with σ^- polarization leads to an expansion of the M^- domain. Note that in sweeping measurements, σ^+ (σ^-) polarization reverses M^- (M^+).

The same results were observed in a Pt/Co/Pt layer exposed to 40-fs laser pulses, as depicted in Fig. 1(b). Laser-induced domain wall motion was obtained in the Pt/Co/Pt single layer only when the laser beam was placed in the vicinity of the DW. In Fig. 1(b), the laser beam spot is centered on the DW,

and the displacement direction of the DW is determined by the helicity of the laser pulses. The same helicity dependence of the DW displacement was seen in the Pt/Co/Pt trilayer with a centered laser beam (see Fig. S1 in the Supplemental Material [29]). Interestingly, to induce DW motion in the Co/Pt single-layer structure a much higher fluence is required than for the Co/Pt trilayer. This can be explained by the pulse-duration dependence of all-optical switching. It was reported in a microscopic model [11] and experimentally proven [14] that deterministic switching is more efficient for longer laser pulses and takes place over a wider range of fluences. Indeed, to obtain AOS with short laser pulses, a higher fluence is necessary [11,14]. Later, we found that the laser-induced DW motion in the Pt/Co/Pt single layer could be canceled with an out-of-plane magnetic field of about 2 Oe whose direction depends on the light helicity that is used. Interestingly, applying 2 Oe perpendicular to the sample was also sufficient to cancel AO-HDS when sweeping circularly polarized light. This field is on the same order of magnitude as what was previously reported for Co/Pt multilayer thin films by Lambert *et al.* [6]. Thus, it is very clear that the direction of the DW displacement depends on the light helicity in all-optical switchable Co/Pt systems and that it corresponds to the reversal direction observed in AO-HDS.

Thereafter, the dynamics of the DW displacement was explored at longer time scales as a function of the distance between the DW and laser beam and laser fluence in $Pt/[Co/Pt]_{x3}/Pt$, as shown in Figs. 2(a) and 2(b). Time-resolved measurements of DW motion were carried out only for the configurations resulting in significant and measurable DW displacement. In Fig. 2(a) right-circular (σ^+) polarization and 2-ps laser pulses were used to observe DW motion for different positions of the center of the laser spot with respect to the DW within an M^- domain. First of all, in Fig. 2(a) one can see that the farther the laser beam is, the greater the final DW displacement is. Second, these plots reveal that the DW motion can be decomposed into three distinct regimes: the DW slowly starts moving; then it experiences a rapid displacement as the DW gets closer to the center of the laser spot, and finally, the speed decreases, and the DW reaches a stable position. The first regime is absent when the center of the beam is on the DW, while the three regimes are clearly observed when the beam is 5 or 8 μm away from the DW. Furthermore, taking the derivative of the time evolution of the DW position, the DW velocity profiles are obtained for all the data presented in Fig. 2 (see Fig. S2 [29]). They distinctly exhibit the three above-discussed regimes (see Fig. S3 [29]). A similar description of the DW velocity regimes could be drawn up with σ^- polarization, as seen in Fig. 2(b) with a beam placed 5 μm within an M^+ domain. Independent of the laser beam position, the maximum velocity is constant and is about 20 μm min^{-1} [see Fig. S2(a)], which corresponds to a displacement of $\sim$0.3 nm per 2-ps pulse for relatively low fluences of 0.04 mJ cm^{-2}. Note that we were limited by the time resolution of 1 s, i.e., 1000 pulses, to calculate the DW velocity.

Moreover, the laser fluence F dependence of the DW motion was studied, as shown in Fig. 2(b). Left-circular (σ^-) polarization was used to induce DW motion, and the beam spot was placed at 5 μm from the DW within an M^+ domain. As depicted in Fig. 2(b), the higher the fluence is, the faster the

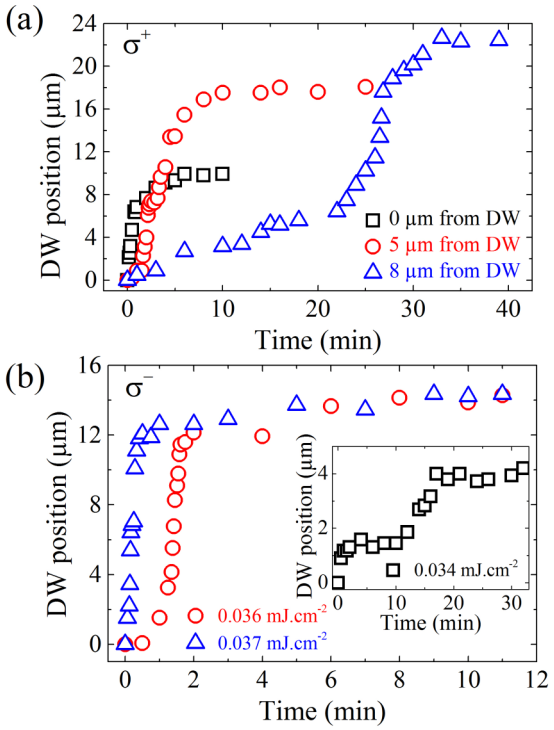

FIG. 2. Time evolution of the domain wall displacement (DWD) in the Co(0.4 nm)/Pt(0.7 nm) trilayer obtained from magneto-optical image recording as a function of (a) laser beam position from the DW and (b) laser fluence upon excitation of a 2-ps laser beam with a repetition rate of 1 kHz. (a) Right-circularly polarized light (σ^+) is used to shine a magnetization-down domain with a fluence of 0.04 mJ cm^{-2} for a laser beam placed at 0, 5, and 8 μm from the DW. (b) The left-circularly polarized (σ^-) laser beam is placed at 5 μm from the DW on a domain with magnetization up with three different laser fluences. Three regimes can be distinguished for the laser-induced DW motion: a slow displacement and depinning of the DW, followed by a dramatic change in the DW position that finally stabilizes.

DW motion is, and the larger the displacement is. Increasing the laser fluence only from 0.034 to 0.037 mJ cm^{-2} leads to a dramatic increase in the maximum DW displacement from 4 to 14 μm and in the peak velocity from 1 to 100 μm min^{-1} [see Fig. S2(b)]. The DW reaches the same final position for $F = 0.036$ and 0.037 mJ cm^{-2}, thus indicating that there is another limiting factor in addition to the laser fluence that controls the maximum DW displacement. This factor is likely to be related to the presence of pinning sites and a distribution of pinning energy in the continuous film. A maximum DW displacement of $\sim$2 nm per 2-ps pulse was achieved for the highest fluence. Note that the fluence window in which significant DW motion is observed is extremely narrow. For a fluence larger than 0.037 mJ cm^{-2}, nucleation started to take place; in contrast for a fluence below 0.034 mJ cm^{-2} no DW displacement was measured. These threshold values may vary over the sample surface due to local defects. In addition, for any laser-beam-DW distance larger than 10 μm, no DW motion was observed at any fluence. This indicates the existence of a power threshold and thus a maximum initial distance between the DW and the center of the laser to achieve DW displacement.

This maximum initial distance is deduced from the abscissa of the power threshold on the Gaussian laser profile. Hence, the study of the DW dynamics allows us to correlate the depinning time to the energy brought by the laser and the beam position, i.e., the spatial energy (temperature) profile that the DW sees. However, such measurements with our experimental setup were not possible for femtosecond-laser-pulse-induced DW motion as the displacement occurs on a time scale that is much shorter than the time resolution of the time-resolved Faraday imaging technique we implemented.

B. Effect of the helicity and linear polarization on the domain wall motion

To understand how DW motion is induced by light, it is important to separate the effects due to the temperature, as the laser brings heat to the sample, and also to the helicity. For this reason we reproduced the same experiments described in Fig. 1 but with linear polarization (π) for which only an increase in the temperature is associated with the optical excitation. The results are shown in Fig. 3(a). In the Pt/Co/Pt single layer, a DW was created and then exposed to linearly polarized light for three different laser beam positions. The exposure time was greater than the one needed to observe DW motion in Fig. 1(b). For a laser beam spot centered on the DW, no motion is observed [Fig. 3(a)]. This can be understood in the sense that the temperature profile with respect to the DW is symmetrical and, consequently, no specific direction for the DW to move in is preferred. However, as seen in Figs. 3(b) and 3(c), when the laser beam is off centered on either the magnetization-up or -down domain, the DW moves towards the center of the laser beam. If the fluence is too low, no significant DW displacement is observed, thus indicating that the energy brought by the laser was not enough to overcome the pinning energy barrier. These findings clearly demonstrate that in the absence of helicity the DW tends to move towards the hottest spot.

Thereafter, we investigated the laser-induced DWD as a function of the degree of light ellipticity ϵ. We measured the farthest stable DW position while gradually changing the angle θ of the QWP, i.e., progressively introducing or reducing helicity in the optical excitation [see Fig. 3(d)]. A domain wall was created in the same material as before. Initially, the center of the laser beam was placed on the DW and the angle of the QWP was set to 0°. The polarization was changed by a step of 10°, and an image with a Faraday microscope was taken only after stabilization of the DW. The results are presented in Fig. 3(d). The DWD is defined as the relative motion of the DW with respect to its initial position. The maximum DWD is reached when the sample is illuminated with circular polarization (σ^+ and σ^-), i.e., $\epsilon = \pi/4$ or $-\pi/4$. Notably, the amplitude of the displacement is almost the same for both helicities; only the direction of the DW motion differs. Yet there is a small shift of the curve that may be attributed to the nonuniform distribution of pinning sites on either side of the DW.

Moreover, when the light has no ellipticity $\epsilon = 0$, i.e., it is linearly polarized, the DW displacement is close to zero, which is in agreement with the findings in Fig. 3(a). In addition, the evolution of the DW position with the polarization can be fitted with a sinusoid, which indicates that the laser-induced DW motion is perfectly reproducible and robust with regard

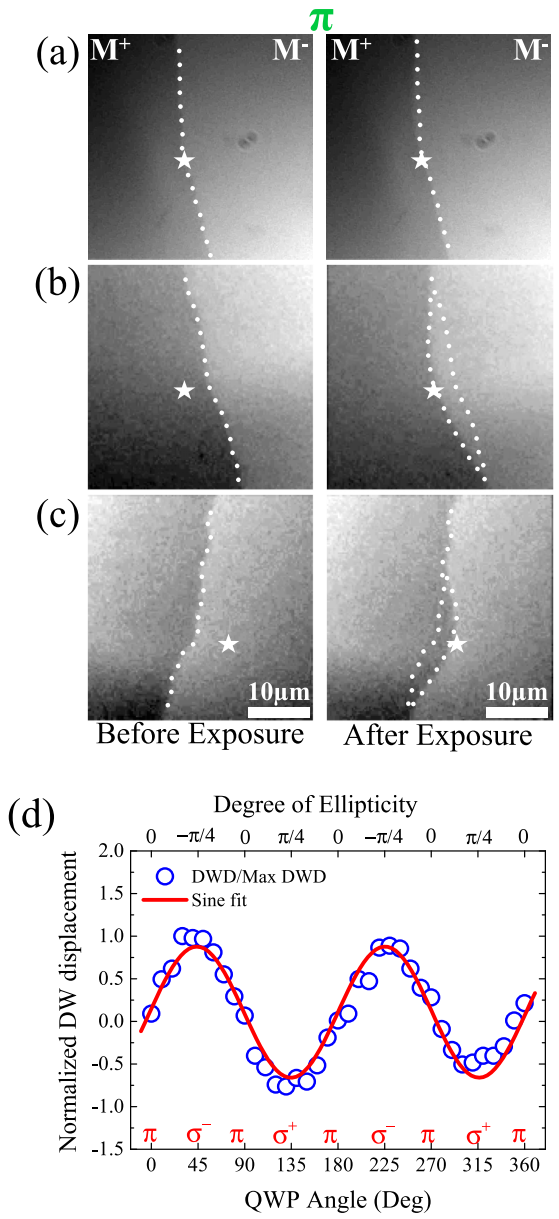

FIG. 3. (a)–(c) Magneto-optical Faraday images of a DW in a Pt(4.5 nm)/Co(0.6 nm)/Pt(4.5 nm) thin film exposed to 40-fs linearly polarized (π) laser pulses with a fluence of 7 mJ cm^{-2}. The laser beam spot (star) is on the DW in (a) and off centered in (b) and (c). The DW moves towards the center of the beam, i.e., the hottest regions, independently of the magnetization direction. (d) Normalized DWD induced by 40-fs laser pulses in Pt(4.5 nm)/Co(0.6 nm)/Pt(4.5 nm) plotted against the angle θ of the quarter-wave plate (QWP) and the degree of light ellipticity ϵ for linear polarization $\epsilon = 0$ and for circular polarization $\pi/4$ or $-\pi/4$. A maximum DW displacement of about 2 μm was obtained. The laser beam is initially centered on the DW at $\theta = 0°$ and kept fixed. The fluence is set to 12.5 mJ cm^{-2}

to the polarization that is used. Figure 3(d) clearly shows that, although circular and linear polarizations bring the same photon energy to the system, the DW ends up in a different potential well. Indeed, as seen in Figs. 3(b) and 3(c), linear polarization brings the DW towards the hottest spot, while circularly polarized light tends to move the DW towards colder

regions, i.e., away from the center of the beam. However, even circularly polarized light brings heat to the sample; therefore, the resulting displacement must be seen as a balance between the effect of helicity and temperature increase. Figure 3(d) shows the competition between the two. Any amount of ellipticity ($\epsilon \neq 0$) introduced in the light induces a displacement that is then balanced by the temperature gradient, which tends to push the DW towards the hottest point, i.e., the center of the laser beam. As the degree of ellipticity increases in absolute (ϵ from 0 to $-\pi/4$), the DW moves farther. By decreasing the light ellipticity (ϵ from $-\pi/4$ to 0), the temperature gradient gradually overcomes the helicity effect, and the DW moves back to its initial position. Thus, these experiments give clear evidence that helicity-dependent all-optical DW motion triggered by laser excitation results from the balance of three contributions, namely, the DW pinning, the effect of the light helicity, and the temperature gradient induced by laser heating.

IV. DISCUSSION

The main results of this study demonstrate that it is possible to have helicity-dependent laser-induced DW motion in Co/Pt multilayer thin films. This corroborates the assumption made for the cumulative two-regime switching process proposed to explain AO-HDS in ferromagnetic Co/Pt films [13,14]. Indeed, starting from a multidomain state, it is now clear that under optical excitation with circularly polarized laser pulses, the DW will move in one direction according to the light helicity, which will result in the shrinkage or growth of domains of opposite magnetization. It is now important to understand the mechanism behind this helicity-dependent laser-induced domain wall motion in Co/Pt.

A. Mechanism for laser-induced domain wall motion

The experimental results in this paper allowed us to determine three contributions that are involved in the DW displacement in Co/Pt induced by femtosecond- and picosecond laser pulses: DW pinning, the temperature gradient across the DW, and the effect of the helicity. To unpin a DW, an energy barrier E_{dep} associated with a depinning field H_{dep} has to be overcome. When the laser fluence was too low, no DWD was observed, thus indicating that the pinning potential was not overcome. As a result, pinning opposes the laser-induced displacement direction. Moreover, exposing the sample to laser pulses generates heating in the material and therefore a temperature gradient across the DW. The influence of the increase of the temperature can be elucidated by studying the effect of linear polarization. Our results prove that the DW moves towards the hottest spot, which is consistent with previous studies that reported DW motion in thermal gradients in ferromagnetic systems [24–26]. Hence, the direction of the DWD is given by the direction of the temperature gradient. In the presence of a symmetric temperature gradient across the wall, e.g., when the laser is centered on the DW, no displacement is observed. However, the effect of circular polarization upon the DW is more ambiguous as σ^+ and σ^- polarizations also bring heat to the sample in addition to angular momentum. Yet a pure helicity effect can be seen for a laser spot centered on the DW since in this configuration heating cannot break the symmetry [see Fig. 1(b)]. In this case, the direction of the displacement induced by the pure helicity effect can be determined.

Let's take the example of σ^+ polarization as seen in Fig. 1(a). When the center of the laser spot is on an M^+ domain, the temperature gradient tends to pull the DW towards the hottest area, i.e., to the left, and the helicity in the other direction. The pinning aims to maintain the DW at the same position. As a result, all the effects cancel each other out, no significant displacement is observed. When σ^+ illuminates an M^- domain, the temperature gradient and the helicity add together and are stronger than the pinning. Thus, they both pull the DW in the same direction. Once the DW crosses the center of the beam spot, the temperature gradient changes direction, and as it keeps moving farther, the temperature gradient and the pinning get stronger and tend to compete with the helicity. Hence, DW motion continues until the equilibrium of the three contributions is reached. This complex interplay between pinning, temperature, and helicity also appears in Fig. 3(d). Since the laser is kept at a fixed position [normalized DWD = 0 in Fig. 3(b)], it is clear that any amount of helicity introduced in the light balances the temperature gradient and the pinning.

B. Models for the effect of the helicity on the domain wall

In this section, we will discuss the microscopic origin of the effect of the helicity and its contribution to the laser-induced DW motion. Several mechanisms explaining AO-HDS in ferromagnetic thin films can be found in the literature based on either the inverse Faraday effect [11] or magnetic circular dichroism [10,12]. Here, we discuss two hypotheses to explain light-induced DW motion based on either athermal or purely thermal effects. First, we decided to test the IFE mechanism. A wide range of estimations for the IFE-induced field from 0.1 to several tens of teslas can be found in the literature [11,30–32]. However, in our experiments we can expect a field value much lower since we used a laser fluence below the switching threshold. Moreover, the laser power was chosen in order to avoid domain nucleation and to have only DW propagation. Thus, we can assume that it is equivalent to applying a low continuous magnetic field to make the DW propagate. To obtain the laser-induced DW displacement under the IFE assumption, we used the Fatuzzo-Labrune model, which allows calculating the DW velocity in the case of magnetization relaxation [see Eq. (1)] [33,34]. The model describes the energy that has to be brought when applying a magnetic field to overcome the pinning barrier E_{dep} and to make the DW move within a given volume, the Barkhausen volume V_{B}. Moreover, the laser beam can be described as a Gaussian distribution of temperature and positive effective magnetic field for σ^+ polarization under the assumption of IFE, as shown in Fig. 4(a). We assume that the center of the laser beam spot corresponds to a maximum temperature of 600 K (300 K above room temperature, RT), close to the Co Curie temperature, and a field of 10 mT:

$$v_{H,T} = v_0 \exp\left(-\frac{E_{\mathrm{dep}} - 2HM_S V_B}{k_B T}\right). \quad (1)$$

This description of the laser beam is implemented in Eq. (1), which gives the DW velocity profile in Fig. 4(a). Each

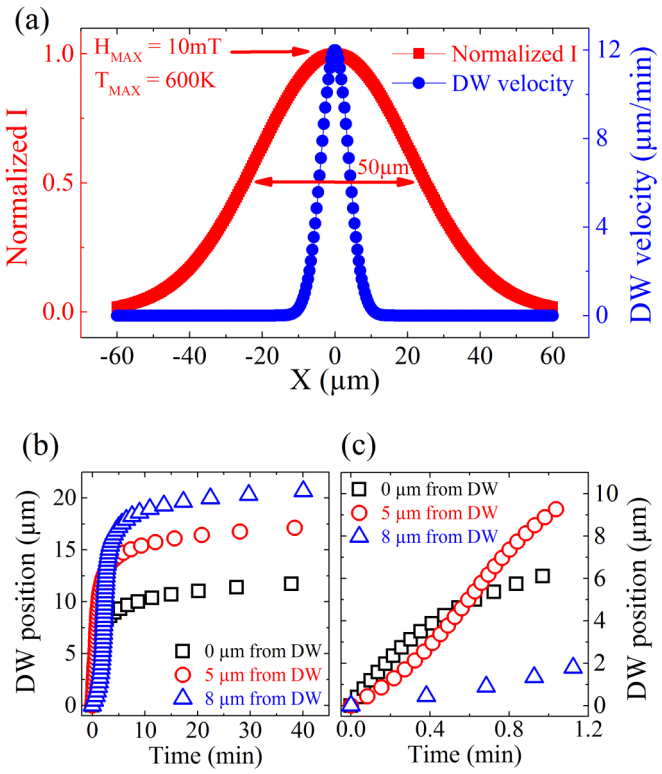

FIG. 4. (a) Simulations of the DW displacement in a $[Co(0.4\ nm)/Pt(0.7\ nm)]_{x3}$ thin film induced by circularly polarized laser pulses modeled as a Gaussian distribution of effective magnetic field and temperature with a maximum intensity of (10 mT, 600 K) and a FWHM of ∼50 μm. (b) and (c) Time evolution of the DW motion for three different distances between the laser beam and the DW based on the Fatuzzo-Labrune model. Similar results for the DW motion as described in Fig. 2 are obtained here.

combination of temperature and effective magnetic field (T, H) at a distance x from the center of the beam generates a displacement $u_{T,H(x)}$ at velocity $v_{T,H(x)}$ calculated from the Fatuzzo-Labrune model. Assuming that the DW velocity is constant over $\delta x \ll 1$, one can deduce $v(t)$ and integrate it to obtain the time evolution of the DW position presented in Figs. 4(b) and 4(c) for the following tested values: $E_{dep} \simeq 65k_B$ RT, $V_B = 9.7 \times 10^{-18}$ cm^{-3}, $v_0 = 1.50 \times 10^{-7}$ m s^{-1}. The model was run for several laser beam positions (0, 5, and 8 μm from the DW). The simulations in Fig. 4(b) provide DW dynamics and results similar to those previously described in Fig. 2. Yet it is noticeable that for a laser beam at 8 μm from the DW, the simulated displacement occurs over a shorter time scale than in Fig. 2(a). This can be explained by the fact that the developed model does not take into account the pulse duration and the laser repetition rate, which are likely to impact the DW dynamics. Note that the simulations are not obtained by fitting our data. Implementing a left-circularly polarized laser (σ^-), i.e., a distribution of negative effective magnetic field leads to a vanishing velocity profile. As a result, helicity-dependent laser-induced DW motion in Pt(4.5 nm)/Co(0.6 nm)/Pt(4.5 nm) was successfully reproduced. Thus, this demonstrates that the effect of the helicity on the DW can, indeed, be described as an athermal effective magnetic field whose direction depends upon the helicity and that the DW displacement arising from this model is in agreement with our experimental data. In order to improve this IFE-based mechanism, one would need to study the laser-induced DW inertia and its dependence upon the pulse duration and laser repetition rate.

Last, one could argue that the DW motion results only from purely thermal effects, namely, MCD in addition to the dc laser heating close to Curie temperature. Since in our experiments the laser beam spot overlaps with two domains of opposite magnetization directions, a difference in absorption of the M^+ and M^- domains would result in an additional temperature gradient across the DW. As already mentioned, it was proven that the DW could effectively move in the presence of thermal gradients [25,26]. When heated locally, a DW must move towards the hottest regions in order to minimize its free energy. Therefore, the temperature gradient acts as an effective field that drives the DW towards the regions with higher temperature if it is greater than the depinning field at the laser temperature [26].

Consequently, here the question is whether a MCD on the order of 0.5%–2% as reported in the literature [12,14] for ferromagnetic materials would induce a sufficient thermal gradient to unpin the DW. According to calculations based on the two-temperature model [35], a MCD of 2% corresponds to a temperature difference of about 10 K. In Co/Pt thin films, the domain wall width is typically in the range of 10 nm. Therefore, the temperature gradient across the DW due to MCD is on the order of 1 K nm^{-1}. One can calculate the effective magnetic field for MCD of 2% using the same model as in Ref. [23] considering, for our Co/Pt structures, a DW with a surface energy σ_S of 8 mJ m^{-2}, a saturation magnetization of $M_S = 1720$ emu cm^{-3}, a Curie temperature of $T_C = 650$ K, an initial temperature $T_0 = 300$ K, and a thermal gradient of about 1 K nm^{-1}. An estimated field of 7 mT is found, which is close to the value used in the previously discussed athermal model and is on the same order of magnitude as depinning fields in Co/Pt thin films [18,36]. Hence, MCD produces a field that can unpin a DW. From the results in Fig. 1(b), to explain the direction of the DW motion based on MCD, σ^+ (σ^-) needs to be more absorbed by an M^- (M^+) domain. In such a case, pumping the DW with σ^+ laser pulses, the temperature would locally be higher in the M^- domain, which would lead to an expansion of the M^+ domain. However, to confirm the role of MCD, it is important to know the actual direction of the temperature gradient and which magnetization state is the least absorbent for both helicities.

Finally, one could argue that spin currents are generated via the spin Seebeck effect arising from the temperature gradient due to laser heating [37,38]. These spin-polarized currents can lead to DW motion via either a charge- or magnon-based spin-transfer torque [39,40]. In this case, the DW is dragged towards hotter regions [40], and considering the MCD, the helicity dependence of the DW displacement can be explained. Indeed, the spin diffusion length in Co (38 ± 12 nm at 300 K [41]) is comparable to or larger than the displacement per pulse we observed.

V. CONCLUSION

In conclusion, we have demonstrated that it is possible to observe helicity-dependent laser-induced domain wall motion

in Co/Pt multilayer thin films, which show all-optical helicity-dependent magnetization switching. The reported domain wall displacement could be achieved with either femtosecond or picosecond laser pulses with a displacement of ∼2 nm per 2-ps pulse. In order to compare it to any other stimuli-based DW motion, DW inertia during the laser pulse has to be studied. Interestingly, it was discovered that the process of domain wall motion induced by light involves the balance of three contributions, the domain wall pinning, the temperature gradient across the DW due to dc laser heating, and the effect of the helicity. The Fatuzzo-Labrune model successfully reproduced the experimental results of the DW displacement, making the inverse Faraday effect a likely explanation for the helicity effect on the DW, while the uncertainty about the direction of the MCD gradient raises doubt about its contribution. To validate the MCD mechanism, all-optical switching must end in the least absorbent state. These findings provide valuable insights into the underlying mechanism of AO-HDS as it was shown that it is intrinsically related to helicity-dependent DW motion.

ACKNOWLEDGMENTS

We would like to thank R. Descoteaux for technical assistance, P. Vallobra for help with the dc magneton sputtering deposition of the samples, and P. Scheid for micromagnetic simulations and modeling. This work was supported partly by the French PIA project Lorraine Université d'Excellence reference ANR-15-IDEX-04-LUE, and NRI, the Office of Naval Research, MURI (Multidisciplinary University Research Initiative) program.

[1] M. S. El Hadri, M. Hehn, G. Malinowski, and S. Mangin, J. Phys. D **50**, 133002 (2017).
[2] A. Kirilyuk, A. V. Kimel, and T. Rasing, Rev. Mod. Phys. **82**, 2731 (2010).
[3] C. D. Stanciu, F. Hansteen, A. V. Kimel, A. Kirilyuk, A. Tsukamoto, A. Itoh, and T. Rasing, Phys. Rev. Lett. **99**, 047601 (2007).
[4] S. Mangin, M. Gottwald, C.-H. Lambert, D. Steil, V. Uhlir, L. Pang, M. Hehn, S. Alebrand, M. Cinchetti, G. Malinowski, Y. Fainman, M. Aeschlimann, and E. E. Fullerton, Nat. Mater. **13**, 286 (2014).
[5] C. Schubert, A. Hassdenteufel, P. Matthes, J. Schmidt, M. Helm, R. Bratschitsch, and M. Albrecht, Appl. Phys. Lett. **104**, 082406 (2014).
[6] C. H. Lambert, S. Mangin, B. S. D. C. S. Varaprasad, Y. K. Takahashi, M. Hehn, M. Cinchetti, G. Malinowski, K. Hono, Y. Fainman, M. Aeschlimann, and E. E. Fullerton, Science **345**, 1337 (2014).
[7] Y. K. Takahashi, R. Medapalli, S. Kasai, J. Wang, K. Ishioka, S. H. Wee, O. Hellwig, K. Hono, and E. E. Fullerton, Phys. Rev. Appl. **6**, 054004 (2016).
[8] I. Radu, K. Vahaplar, C. Stamm, T. Kachel, N. Pontius, H. A. Durr, T. A. Ostler, J. Barker, R. F. Evans, R. W. Chantrell, A. Tsukamoto, A. Itoh, A. Kirilyuk, T. Rasing, and A. V. Kimel, Nature (London) **472**, 205 (2011).
[9] T. A. Ostler, J. Barker, R. F. L. Evans, R. W. Chantrell, U. Atxitia, O. Chubykalo-Fesenko, S. El Moussaoui, L. Le Guyader, E. Mengotti, L. J. Heyderman, F. Nolting, A. Tsukamoto, A. Itoh, D. Afanasiev, B. A. Ivanov, A. M. Kalashnikova, K. Vahaplar, J. Mentink, A. Kirilyuk, T. Rasing, and A. V. Kimel, Nat. Commun. **3**, 666 (2012).
[10] A. R. Khorsand, M. Savoini, A. Kirilyuk, A. V. Kimel, A. Tsukamoto, A. Itoh, and T. Rasing, Phys. Rev. Lett. **108**, 127205 (2012).
[11] T. D. Cornelissen, R. Córdoba, and B. Koopmans, Appl. Phys. Lett. **108**, 142405 (2016).
[12] J. Gorchon, Y. Yang, and J. Bokor, Phys. Rev. B **94**, 020409 (2016).
[13] M. S. El Hadri, P. Pirro, C.-H. Lambert, S. Petit-Watelot, Y. Quessab, M. Hehn, F. Montaigne, G. Malinowski, and S. Mangin, Phys. Rev. B **94**, 064412 (2016).
[14] R. Medapalli, D. Afanasiev, D. K. Kim, Y. Quessab, S. Manna, S. A. Monotoya, A. Kirilyuk, Th. Rasing, A. V. Kimel, and E. E. Fullerton, Phys. Rev. B **96**, 224421 (2017).
[15] S. S. P. Parkin, M. Hayashi, and L. Thomas, Science **320**, 190 (2008).
[16] M. Hayashi, L. Thomas, R. Moriya, C. Rettner, and S. S. P. Parkin, Science **320**, 209 (2008).
[17] D. A. Allwood, G. Xiong, C. C. Faulkner, D. Atkinson, D. Petit, and R. P. Cowburn, Science **309**, 1688 (2005).
[18] P. J. Metaxas, J. P. Jamet, A. Mougin, M. Cormier, J. Ferre, V. Baltz, B. Rodmacq, B. Dieny, and R. L. Stamps, Phys. Rev. Lett. **99**, 217208 (2007).
[19] G. Malinowski, O. Boulle, and M. Kläui, J. Phys. D **44**, 384005 (2011).
[20] I. M. Miron, T. Moore, H. Szambolics, L. D. Buda-Prejbeanu, S. Auffret, B. Rodmacq, S. Pizzini, J. Vogel, M. Bonfim, A. Schuhl, and G. Gaudin, Nat. Mater. **10**, 419 (2011).
[21] T. H. E. Lahtinen, K. J. A. Franke, and S. Van Dijken, Sci. Rep. **2**, 258 (2012).
[22] P. M. Shepley, A. W. Rushforth, M. Wang, G. Burnell, and T. A. Moore, Sci. Rep. **5**, 7921 (2015).
[23] J. Torrejon, G. Malinowski, M. Pelloux, R. Weil, A. Thiaville, J. Curiale, D. Lacour, F. Montaigne, and M. Hehn, Phys. Rev. Lett. **109**, 106601 (2012).
[24] J.-P. Tetienne, T. Hingant, J.-V. Kim, L. Herrera Diez, J.-P. Adam, K. Garcia, J.-F. Roch, S. Rohart, A. Thiaville, D. Ravelosona, and V. Jacques, Science **344**, 1366 (2014).
[25] S. Moretti, V. Raposo, E. Martinez, and L. Lopez-Diaz, Phys. Rev. B **95**, 064419 (2017).
[26] F. Schlickeiser, U. Ritzmann, D. Hinzke, and U. Nowak, Phys. Rev. Lett. **113**, 097201 (2014).
[27] M. Bersweiler, K. Dumesnil, D. Lacour, and M. Hehn, J. Phys. Condens. Matter **28**, 336005 (2016).
[28] M. S. El Hadri, P. Pirro, C.-H. Lambert, N. Bergeard, S. Petit-Watelot, M. Hehn, G. Malinowski, F. Montaigne, Y. Quessab, R. Medapalli, E. E. Fullerton, and S. Mangin, Appl. Phys. Lett. **108**, 092405 (2016).
[29] See Supplemental Material at http://link.aps.org/supplemental/10.1103/PhysRevB.97.054419 for figures showing DW motion in the Co/Pt trilayer with a centered 2-ps laser beam and the DW velocity profiles exhibiting the three distinct regimes.

[30] A. V. Kimel, A. Kirilyuk, P. A. Usachev, R. V. Pisarev, A. M. Balbashov, and Th. Rasing, Nature (London) **435**, 655 (2005).
[31] M. O. A. Ellis, E. E. Fullerton, and R. W. Chantrell, Sci. Rep. **6**, 30522 (2016).
[32] R. John, M. Berritta, D. Hinzke, C. Müller, T. Santos, H. Ulrichs, P. Nieves, J. Walowski, R. Mondal, O. Chubykalo-Fesenko, J. McCord, P. M. Oppeneer, U. Nowak, and M. Münzenberg, Sci. Rep. **7**, 4114 (2017).
[33] E. Fatuzzo, Phys. Rev. **127**, 1999 (1962).
[34] M. Labrune, S. Andrieu, F. Rio, and P. Bernstein, J. Magn. Mater. **80**, 211 (1989).
[35] J. Mendil, P. Nieves, O. Chubykalo-Fesenko, J. Walowski, T. Santos, S. Pisana, and M. Münzenberg, Sci. Rep. **4**, 3980 (2014).
[36] J. Gorchon, S. Bustingorry, J. Ferre, V. Jeudy, A. B. Kolton, and T. Giamarchi, Phys. Rev. Lett. **113**, 027205 (2014).
[37] H. Adachi, K.-I. Uchida, E. Saitoh, and S. Maekawa, Rep. Prog. Phys. **76**, 036501 (2013).
[38] G.-M. Choi, C.-H. Moon, B.-C. Min, K.-J. Lee, and D. G. Cahill, Nat. Phys. **11**, 576 (2015).
[39] K. M. D. Hals, A. Brataas, and G. E. W. Bauer, Solid State Commun. **150**, 461 (2010).
[40] D. Hinzke and U. Nowak, Phys. Rev. Lett. **107**, 027205 (2011).
[41] L. Piraux, S. Dubois, A. Fert, and L. Belliard, Eur. Phys. J. B **4**, 413 (1998)